

Structure of glassy lithium sulfate films sputtered in nitrogen (LISON): Insight from Raman spectroscopy and ab initio calculations

Christian R. Müller,¹ Patrik Johansson,² Maths Karlsson,² Philipp Maass,¹ and Aleksandar Matic²

¹*Institut für Physik, Technische Universität Ilmenau, 98684 Ilmenau, Germany*

²*Department of Applied Physics, Chalmers University of Technology, 41296 Göteborg, Sweden*

(Dated: November 28, 2018)

Raman spectra of thin solid electrolyte films obtained by sputtering a Li_2SO_4 target in nitrogen plasma are measured and compared to ab initio electronic structure calculations for clusters composed of 28 atoms. Agreement between measured and calculated spectra is obtained when oxygen atoms are replaced by nitrogen atoms and when the nitrogen atoms form bonds with each other. This suggests that the incorporation of nitrogen during the sputtering process leads to structures in the film, which prevent crystallization of these thin film salt glasses.

PACS numbers: 66.30.Dn, 66.30.Hs

I. INTRODUCTION

Glassy thin film electrolytes are materials of considerable technological interest. They are used in the design of modern solid state batteries, electrochemical sensors, supercapacitors, and electrochromic devices. Most of the materials nowadays are fabricated using the sol-gel methods, but new possibilities are currently explored by using sputtering techniques. An example are thin films produced by sputtering a $0.75\text{Li}_2\text{O}-0.25\text{P}_2\text{O}_5$ target in a nitrogen plasma (LIPON,¹), which show ionic conductivities of about $3 \times 10^{-6} \Omega^{-1}\text{cm}^{-1}$. This material has been successfully used in microbatteries² and electrochromic systems.³ Through the mixed network former effect the ionic conductivity could be further increased to about $9 \times 10^{-6} \Omega^{-1}\text{cm}^{-1}$ by taking a $0.75\text{Li}_2\text{O}-0.25[0.2\text{SiO}_2-0.8\text{P}_2\text{O}_5]$ target.⁴

The sputtering technique is in particular interesting, since it extends the glass forming range. This has recently been observed in the ternary $\text{Li}_2\text{O}-\text{B}_2\text{O}_3-\text{Li}_2\text{SO}_4$ systems,⁵ where the sulfate content could be increased to amounts that would lead to crystallization when preparing glass by melt quenching. In fact, the borate component can be fully eliminated by sputtering a Li_2SO_4 target in a nitrogen containing plasma, leading to an amorphous material referred to as LISON.⁶ With respect to the target material, one could speak of a “salt glass”. It is also found that sputtering in argon plasma does not lead to an amorphous film, indicating that nitrogen plays a crucial role in the glass forming ability. Indeed, it was shown that nitrogen is partly incorporated into the material⁶ with a sulphur to nitrogen ratio of about 2:1. At present it is not clear how the structure of these salt glasses is built up, in particular in which way the incorporation of nitrogen takes place and how this leads to a stabilization of the amorphous structure.

The aim of this work is to get insight in the structural arrangements of this new glass system, how the nitrogen is incorporated in the structure and how this is related to the increased stability of the material towards crystallization. To this end we study LISON films by Raman

spectroscopy and compare the experimental vibrational spectra with predictions from ab initio electronic structure calculations based on density functional theory. Calculations have been performed for pure Li_2SO_4 clusters and nitrogen doped Li_2SO_4 clusters.

II. EXPERIMENTAL

The Raman experiments were performed at room temperature in argon atmosphere using a micro-Raman setup with an argon-krypton laser tuned to the 514 nm line as excitation source. With this experimental set-up we have a depth resolution of 14 μm . The power at the sample was 21 mW for the depolarized configuration (perpendicular direction of polarization of the incoming beam with respect to the polarizer in front of the detector) and 7 mW for polarized configuration. The integration time of a single measurement was 300 s. The analysis of the spectrum is based on the median of 27 spectra. Measurements on different spots of the sample gave the same spectrum, showing that the film was homogeneous.

The LISON film had a thickness of 4 μm and was prepared by sputtering a Li_2SO_4 target in nitrogen plasma at pressure 1 Pa.⁷ Due to the rather strong Raman response of the silicon substrate and the small thickness of the film, the measured spectra are dominated by the silicon signal. In order to obtain the response of the film, a reference spectrum from a clean silicon substrate was subtracted. In this procedure it was important to ensure that the substrate had the same orientation with respect to the incident polarization, wherefore we made use of the polarization dependence of the intensity of the 521 cm^{-1} Raman line of silicon.

III. AB INITIO CALCULATIONS

Electronic structure calculations were performed for Li_2SO_4 clusters with 28 atoms (4 Li_2SO_4 units). Start configurations were created based on the conception that

the lithium sulfate salt glass consists of intact SO_4 units with lithium ions in between. Using the GaussView3.0 program,⁹ SO_4 tetrahedra were constructed with random orientation. Lithium ions were added under the constraint of minimum interatomic distance of 1.6 Å.

The starting configurations were geometry optimized using the Gaussian03 suite of quantum chemistry programs¹⁰ (for the theoretical background underlying the methods see¹¹). First, the semi-empirical PM3 method was applied, followed by a Hartree Fock calculation with the 6-31G* basis set. These calculations took about 200 CPUh and ~ 200 iterations. For the final optimization using the hybrid density functional B3LYP and the same basis set only a few iterations were needed.

In order to monitor the influence of nitrogen, modified Li_2SO_4 clusters were generated by replacing oxygen atoms by nitrogen atoms in the optimized Li_2SO_4 cluster configurations. These modified clusters were again optimized by employing Hartree Fock and B3LYP with the 6-31G* basis set.

From the 2nd and 3rd order derivatives of the potential energy surface (PES) at the minima found for the optimized configurations, the Raman spectra were calculated. It is clear that the amorphous film will exhibit a large number of local structures corresponding to different minima of the PES. By optimizing different starting configurations it is possible to scan a part of the PES and find minima, whose associated clusters are good representatives of the local structures of the LISON film. This is evaluated by comparing calculated vibrational spectra with the experimental.

IV. EXPERIMENTAL RESULTS

Figure 1 shows (a) the polarized and (b) depolarized Raman spectra for the LISON film. The bare silicon (dashed line) and the sample spectrum (film plus substrate, solid line) are shown in the insets of Figs. 1a,b. The bare silicon spectrum was scaled to fit the characteristics between 250 cm^{-1} and 350 cm^{-1} . The main feature of the resulting difference spectra in Figs. 1a,b is a band between 900 cm^{-1} and 1035 cm^{-1} . A second weaker band is found at 1225 cm^{-1} with a shoulder at slightly lower frequencies, around 1150 cm^{-1} , in the polarized spectrum in Fig. 1a. In addition two more bands may be discerned at 415 cm^{-1} and at 645 cm^{-1} , in particular in the case of the polarized spectrum, where the intense silicon mode at 521 cm^{-1} is absent and does not hamper the subtraction procedure. The intensity gap between 440 cm^{-1} and 500 cm^{-1} in the depolarized spectrum results from the fact that, in order to resolve the weak difference signals, the integration time had to be chosen sufficiently large. As a consequence the intensity of the silicon mode at 521 cm^{-1} present in the depolarized spectrum (see inset in Fig. 1b) saturates the detector in this spectral region.

In order to assign the bands originating from the LI-

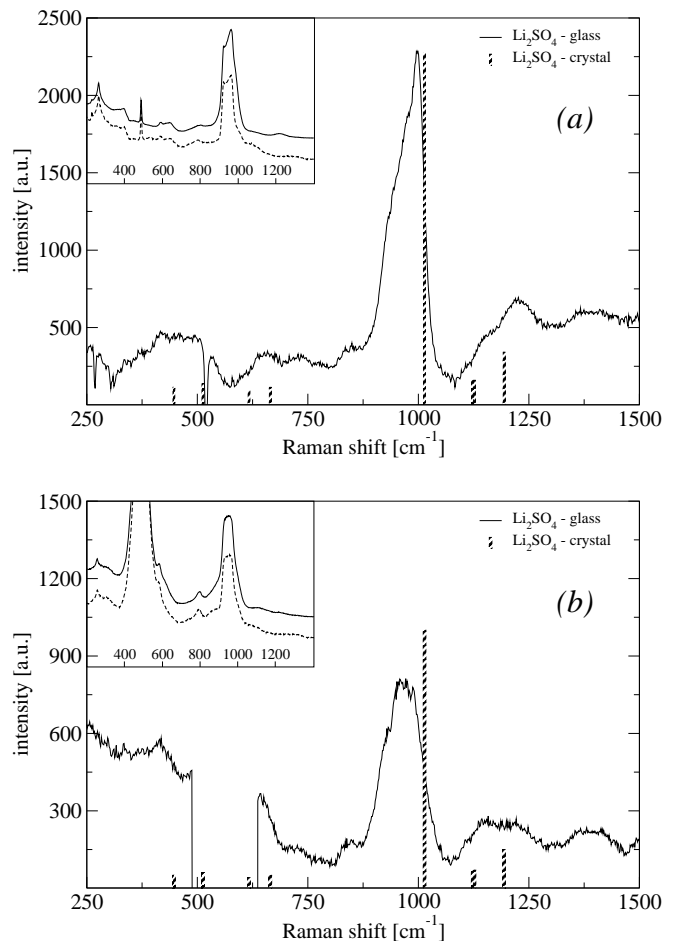


FIG. 1: (a) Polarized and (b) depolarized difference Raman spectra of LISON films on a silicon substrate. The difference signal is obtained by subtracting the spectrum of a bare silicon substrate from the spectrum of the sample. Inset shows the raw data from the sample and the substrate (dashed lines silicon, solid lines LISON film sample). The spectra have been offset for clarity.

SON film in the difference spectra in Fig. 1 we compare the results to the Raman modes found in crystalline Li_2SO_4 ,⁸ marked as bars in the figure. The Raman spectrum of the crystal is dominated by the symmetric breathing mode of SO_4^{2-} at 1014 cm^{-1} , which either is very weak or found at lower frequencies in the glassy film. That this main band covers a range of frequencies where there are no corresponding modes from the crystal, suggests that the structure of the amorphous LISON film and the Li_2SO_4 crystal are different also on the short range order scale. The modes at 1123 cm^{-1} and 1127 cm^{-1} in the crystal (appearing as a single bar in Figs. 1a,b due to their small separation), as well as the mode at 1194 cm^{-1} seem on the other hand to be shifted to higher frequencies and can be related to the bands around 1150 cm^{-1} and around 1225 cm^{-1} in the experimental spectrum. Similarly, the two bands in the film around 415 cm^{-1} and 645 cm^{-1} have likely their

origin in the pair of modes at 447 cm^{-1} , 513 cm^{-1} and the pair of modes at 617 cm^{-1} , 665 cm^{-1} in the crystal, respectively.

V. THEORETICAL RESULTS AND COMPARISON WITH THE EXPERIMENT

For the comparison of the experimental and calculated spectra we will exclusively use the polarized Raman spectrum shown in Fig. 1a, as it is not disturbed by the silicon mode at 521 cm^{-1} . To obtain a smooth spectrum from the calculated Raman lines, each line j with Raman shift ω_j and intensity I_j is replaced by a Gaussian peak function $I_j \exp[-(\omega - \omega_j)^2/\Delta^2]$ with $\Delta = 20\text{ cm}^{-1}$.

In addition, a rescaling of the calculated Raman shifts is in general necessary to obtain good agreement with the experimental spectra, depending on the particular material and method used. Commonly used literature data for these rescaling factors exist for some gas and organic molecules. They have been determined by adjusting calculated to measured frequencies for well defined modes. In our case such literature data are not available and we have to determine the rescaling factor by other means. To do this we focus on the SO_4 breathing mode of the crystal, since one should expect it to be present also in the clusters and the film (although, possibly, with reduced intensity). The calculated SO_4 breathing mode frequencies differ slightly from each other due to the different local surroundings of the SO_4^{2-} anions in the clusters. Taking the average of them and determining the quotient with the corresponding crystal mode frequency gives a stretching factor of 1.11. Using this factor yields theoretical spectra which appear to be shifted to higher frequencies. An optimal overlap of calculated and measured spectra is obtained with a slightly reduced factor of 1.09. This minor correction should not be surprising as some shift of the breathing mode frequency can be expected when considering the crystal and the film. To summarize, for the comparison all calculated spectra are stretched by this factor of 1.09.

A. Li_2SO_4 clusters

Figure 2 shows the Raman spectra calculated from two optimized Li_2SO_4 cluster configurations (dotted and dashed lines) in comparison with the measured Raman spectrum (solid line).

As can be seen from the figure, the calculated spectra for the two different optimized clusters do not deviate much. This can be interpreted in the way that local arrangements participating in the dominating vibrations are still determined by the Li^+ and SO_4^{2-} ions and their mutual Coulomb interaction as in the crystal. As a consequence, the SO_4^{2-} units are rather weakly coupled.

In comparison to the measured Raman spectrum, the calculated ones resemble the overall band structure.

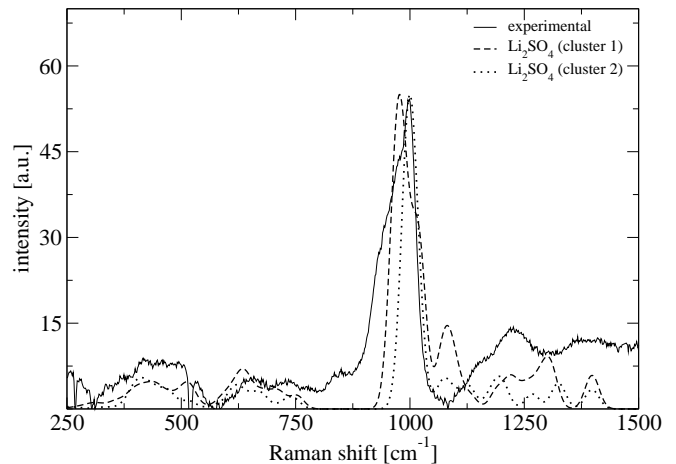


FIG. 2: Comparison of two calculated Raman spectra for Li_2SO_4 clusters with the experimental Raman data.

However, there are two important differences: (i) The experimental spectrum shows a broad shoulder towards lower frequencies from the main band at 1002 cm^{-1} down to 900 cm^{-1} . As there exists not a single vibrational mode between 760 cm^{-1} and 960 cm^{-1} , this shoulder is absent in the calculated spectra. (ii) In the calculated spectra there is intensity due to a mode at 1080 cm^{-1} , while almost no intensity is seen around this frequency in the experimental spectrum. As a first hypothesis deviation (ii) might be related to the finite size of the calculated cluster. A closer inspection of the eigenvector belonging to this mode reveals that it contains an oxygen atom, which moves in the normal direction of the surface of the cluster. Accordingly, this mode can be attributed to an artefact of the limited cluster size.

Deviation (i) on the other hand might be due to structural changes when nitrogen is incorporated in the structure, which can be investigated by comparing experimental spectra to calculated spectra from the nitrogen containing clusters.

B. $\text{Li}_2\text{SO}_4\text{-N}$ (LISON) clusters

The substitution of two oxygen atoms by nitrogen atoms in a cluster has a strong effect on the calculated spectra, as can be seen from Fig. 3, where spectra of 4 different clusters (labeled 1-4 in the figure) are compared to the measured Raman spectrum. This is not surprising as half of the SO_4^{2-} are replaced by SO_3N^{3-} . The rather large amount of nitrogen correspond to results from Rutherford backscattering experiments which yielded a ratio of about 2:1 of sulfur to nitrogen¹² and are also in agreement with previously reported values.⁶

A number of new bands appear in the calculated spectra from the nitrogen containing clusters. However, while the clusters without nitrogen lead to very similar spectra, the modified systems show pronounced differences.

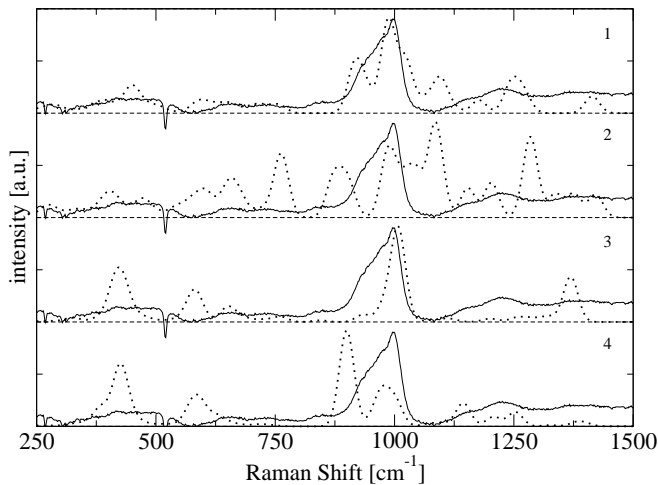


FIG. 3: Comparison of four calculated Raman spectra (dotted lines) for LISON clusters with the experimental Raman data (solid lines).

In general the spectra 2-4 do not compare well with the experimental data, while the calculated spectrum 1 is surprisingly close to the experimental data. In particular, the broad shoulder of the main band is here well reproduced. The additional band at 1080 cm^{-1} is still present, but does not relate to nitrogen incorporation as discussed above. It is interesting to note that the optimal cluster 1 does not only compare most favorably with the experimental spectrum, but also has the lowest energy (1.9 eV lower than the next lowest energy cluster associated with spectrum 3).

Figure 4 shows the atomic configuration of the optimal cluster 1. In contrast to the clusters 2-4, it contains an interaction between two nitrogen atoms in close proximity at a distance of 1.47 \AA , which serves as a type of bridge between the two SO_3N pseudo-tetrahedra. This suggests that the incorporation of nitrogen triggers the formation of structures, which, by hindering a reorientation of the anions relative to each other, prevent the crystallization of the film (or, more precisely, increases the free energy barrier for crystallization).

VI. CONCLUSIONS

By comparing experimental and calculated Raman spectra for LISON systems, we are able to show that

a good representation of an amorphous LISON film is possible using small atomic clusters. Our investigations reveal that in the LISON structure nitrogen is replacing oxygen in the SO_4^{2-} tetrahedra. In the configuration that results in Raman spectra in agreement with the experimental data we find a nitrogen-nitrogen bridge between two anions. This might be the underlying reason for the prevention of crystallization of the LISON material during the sputtering process, as these nitrogen bridges restrain the reorientation of the anions and therefore stabilize an amorphous film structure.

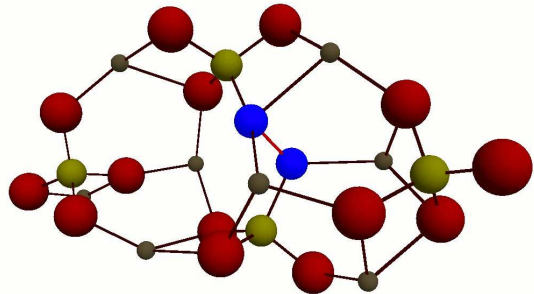


FIG. 4: Atomic configuration of the optimal LISON cluster (corresponding to spectrum 1 in Fig. 3). Oxygen atoms are marked in red (dark gray, large spheres), sulfur atoms in yellow (light gray, mid-size spheres), nitrogen atoms in blue (dark grey, mid-size spheres), and Li atoms in silver (grey, small spheres).

Acknowledgments

We thank Yohann Hamon and Philippe Vinatier from École Nationale Supérieure de Chimie et Physique de Bordeaux, France, for providing the LISON samples, and Efstratios Kamitsos from the Theoretical and Physical Chemistry Institute of the National Hellenic Research Foundation, Athens, Greece, for valuable discussions. Financial support by the HI-CONDELEC EU STREP project (NMP3-CT-2005-516975) is gratefully acknowledged.

¹ X. Yu, J. B. Bates, G. E. Ellison Jr., and F. X. Hart, *J. Electrochem. Soc.* **144**, 524 (1997).
² Y. S. Park, S. H. Lee, B. I. Lee, and S. K. Joo, *Electrochem. Solid State* **2**, 58 (1999).
³ A. Gerouki and R. Goldner, *Mat. Res. Soc. Symp. Proc.* **548**, 679 (1999).

⁴ S. J. Lee, A. K. Baik, and S. M. Lee, *Electrochem. Commun.* **5**, 32 (2003).
⁵ K. H. Joo, P. Vinatier, B. Pecquenard, A. Levasseur, and H. J. Sohn, *Solid State Ionics* **160**, 51 (2003).
⁶ K. H. Joo, H. J. Sohn, P. Vinatier, B. Pecquenard, and A. Levasseur *Electrochem. and Solid State Lett.* **7** (8), A256

(2004).

- ⁷ The sample was prepared at École Nationale Supérieure de Chimie et Physique de Bordeaux.
- ⁸ E. Cazzanelli and R. Frech, *J. Chem. Phys.* **79**, 2615 (1983); *ibid.* **81**, 4729 (1984); only the modes belonging to the A_g symmetry are considered (other representations have slightly shifted modes, but the size of the corresponding shifts are negligible in comparison with the width of the peaks obtained for the film).
- ⁹ GaussView, Version 3.09, R. Dennington II, T. Keith, J. Millam, K. Eppinnett, W. L. Hovell, and R. Gilliland, Semichem, Inc., Shawnee Mission, KS, 2003.
- ¹⁰ Gaussian 03, Revision C.02, M. J. Frisch, G. W. Trucks, H. B. Schlegel, G. E. Scuseria, M. A. Robb, J. R. Cheeseman, J. A. Montgomery, Jr., T. Vreven, K. N. Kudin, J. C. Burant, J. M. Millam, S. S. Iyengar, J. Tomasi, V. Barone, B. Mennucci, M. Cossi, G. Scalmani, N. Rega, G. A. Petersson, H. Nakatsuji, M. Hada, M. Ehara, K. Toyota, R. Fukuda, J. Hasegawa, M. Ishida, T. Nakajima, Y. Honda, O. Kitao, H. Nakai, M. Klene, X. Li, J. E. Knox, H. P. Hratchian, J. B. Cross, V. Bakken, C. Adamo, J. Jaramillo, R. Gomperts, R. E. Stratmann, O. Yazyev, A. J. Austin, R. Cammi, C. Pomelli, J. W. Ochterski, P. Y. Ayala, K. Morokuma, G. A. Voth, P. Salvador, J. J. Dannenberg, V. G. Zakrzewski, S. Dapprich, A. D. Daniels, M. C. Strain, O. Farkas, D. K. Malick, A. D. Rabuck, K. Raghavachari, J. B. Foresman, J. V. Ortiz, Q. Cui, A. G. Baboul, S. Clifford, J. Cioslowski, B. B. Stefanov, G. Liu, A. Liashenko, P. Piskorz, I. Komaromi, R. L. Martin, D. J. Fox, T. Keith, M. A. Al-Laham, C. Y. Peng, A. Nanayakkara, M. Challacombe, P. M. W. Gill, B. Johnson, W. Chen, M. W. Wong, C. Gonzalez, and J. A. Pople, Gaussian, Inc., Wallingford CT, 2004.
- ¹¹ C. J. Cramer, *Essentials of Computational Chemistry* (John Wiley and Sons, Hoboken, New Jersey, 2004).
- ¹² Y. Hamon and P. Vinatier, private communication .